Stress-Induced Crystallization of Biaxially Oriented Polypropylene

Wei Yang, Zhong-Ming Li, Bang-Hu Xie, Jian-Min Feng, Wei Shi, Ming-Bo Yang

State Key Laboratory of Polymer Materials Engineering, College of Polymer Science and Engineering, Sichuan University, Chengdu, 610065, Sichuan, People's Republic of China

Received 30 April 2002; accepted 9 September 2002

ABSTRACT: The hot stretching of thick, extruded sheets at high temperatures is a very important process in the production of finished biaxially oriented polypropylene (BOPP) films with special inner structures. Through a simulation of hot stretching in the machine direction (MD) of the processing of BOPP films, it was found that at high temperatures, the stretching ratio greatly influenced the obtained crystalline structure, as observed by differential scanning calorimetry (DSC). Also, in MD hot stretching, the crystallinity increased by an average of 20%. Wide-angle X-ray diffraction patterns of extruded sheet samples with and without stretching confirmed the structural changes shown by DSC, and the results proved that β-crystal modification did not occur during the MD hot-stretching process.
 J Appl Polym Sci 89: 686–690, 2003

Key words: biaxiality; poly(propylene) (PP); crystallization

INTRODUCTION

Biaxially oriented polypropylene (BOPP) film is a widely used transparent packaging material developed in the 1960s through the mass production of polypropylene (PP) resins. Its advantageous properties include low density, no toxicity, good moisture resistance, good mechanical strength, and dimensional stability and printability.[1–3]

The BOPP resin of isotactic polypropylene (iPP), the molecular chains of which take the 3_1 helical configuration, show rich crystalline structures of α, β, γ, and δ modifications under different processing conditions.[4] Among these modifications, α and β are commonly observed. α modification is the most common and stable and is obtained when PP crystallizes at about 138°C. Although every molecular chain in PP α modification has a 3_1 helical symmetry, the bulk crystalline structure does not present triple symmetry, which is necessary for α modification. β modification, different in its physical and mechanical properties from α modification to some degree, is obtained at about 130°C, the most favorable temperature for β growth,[5–8] and a high content of β crystals can be acquired under special conditions, such as the quenching of the melt within a certain temperature range,[9,10] directional crystallization in a temperature gradient field,[11] shear-induced crystallization,[12] or doping of the resin with certain heterogeneous nucleating agents.[13–15]

Previous publications have commonly reported that β modification is less stable than α modification, tending to transform into α modification when heated within a certain temperature range[16] or stretched.[17] Compared with α modification, β modification is more ductile and easier to stretch, and it has a higher Vicat softening temperature, whereas the tensile yield strength of α modification is higher, the neck formation in a stress–strain test is more obvious, and the strain hardening is delayed.[18]

Commercial BOPP films have special inner structures obtained by the stretching of the thick, extruded sheets at high temperatures in the machine direction (MD) and in the transverse direction. This is the most important stage for controlling the BOPP structures in the whole process.[19] Accordingly, studies on physical problems such as deformation, crystallization, orientation, and rheology during the stretching of extruded sheets are of great importance, both in theory and in practice. The wide-angle X-ray diffraction (WAXD) patterns of the tenter process BOPP film, the tube process BOPP film, and the tenter process extruded sheet are shown in Figure 1. The (300) peak characteristic of β-crystal modification is present in either the tenter process film or the tube process film. However, the tenter process extruded sheet gives a pure α-crystal diffraction pattern. Obviously, the existence of a crystal transition and the stage at which the β crystal comes into being are of great interest. This article focuses on the crystallization of the extruded sheet during MD stretching.

Correspondence to: M.-B. Yang (yangmb@scu.edu.cn).
Contract grant sponsor: Special Funds for Major Research; contract grant sponsor: G1999064805.

Journal of Applied Polymer Science, Vol. 89, 686–690 (2003)

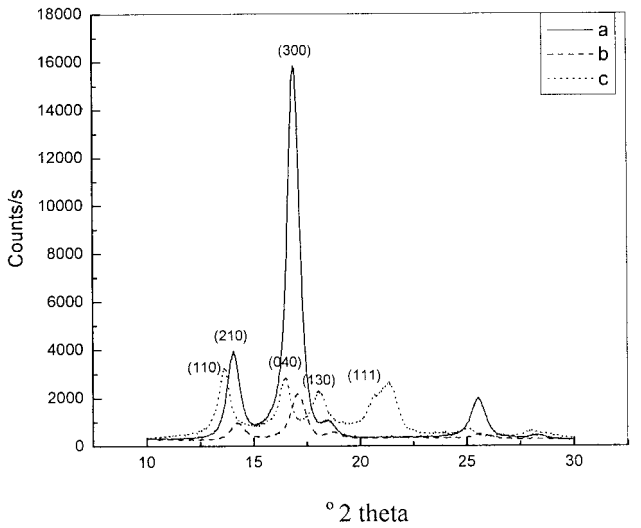

Figure 1 WAXD patterns of the (a) tenter process BOPP film, (b) the tube process BOPP film, and (c) the tenter process extruded sheet.

As mentioned previously, the isothermal and nonisothermal crystallizations of PPs of different grades have been studied in detail. However, for the crystallization behavior of BOPP, especially under practical process conditions, pertinent literature can rarely be found. For this work, through the simulation of the first stage of the extrudate stretching (MD hot stretching), the general crystallization behavior of the BOPP resin was studied.

EXPERIMENTAL

Material

The main material used in this study, PP_{PD382}, was a commercial grade of the BOPP resin with an isotacticity of 93.8%; it was supplied as pellets by Himont Co. (Thailand) with a melt-flow rate of 2.88 g/10 min at 230°C, exerting a force of 21.6 N.

Preparation and stretching of the extruded BOPP sheet

An SJ-20A single-screw extruder (Shanghai Light Machine and Models Co., Shanghai, China), with a screw diameter of 20 mm and a length/diameter ratio of 25, was used to extrude sheets into cold water at 25°C under typical factory conditions. The temperatures from the hopper to the die were 180, 210, 230, and 250°C, and the screw rotation was maintained at 40 rpm. The extruded sheets were machined into 30 mm × 70 mm samples. The samples were stretched at temperatures of 120, 130, and 140°C in a temperature-controlled box setting on an electrical versatile test machine with crosshead speeds of 150, 300, and 450 mm/min and stretching ratios (referring to the elongation divided by the original marked lengths of the samples in this article) of 100, 388, and 471%, respectively. The stretched samples were then quenched in a saturated NaCl solution of ice and water, the temperature of which was kept at about −4°C to minimize postchange of the chain segments and to maintain the morphology obtained over the course of stretching.

Differential scanning calorimetry (DSC)

The DSC analysis was carried out on a TA 2100 Thermal Analysis DSC thermoanalyzer (TA Co., New York) at a heating rate of 10°C/min with 50 mL/min N_2 protection. The thermograms served to determine the heat of fusion (ΔH_f). The degree of crystallinity [ω_c (DSC)] was determined according to the following equation:[20] ω_c (DSC) = $\Delta H_f/\Delta H_0$. ΔH_0 is the ideal heat of fusion of iPP (138 J/g).[21]

WAXD

WAXD patterns were obtained in a Philips X'Pert Graphics & Identify instrument (The Netherlands) operating at 50 kV and 30 mA with Ni-filtered Cu Kα radiation.

RESULTS AND DISCUSSION

DSC

Figures 2–5 show the superimpositioning of DSC thermograms recorded at the same heating rate (10/min^{-1}) for extruded sheets without stretching and for samples drawn under different conditions. For Figures 2–4, the stretching temperature is 140°C, and the stretching velocities are 150, 300, and 450 mm/min, respectively. In these figures, the curves are for different tensile ratios, which are labeled 200, 388, and 471%, whereas for Figure 5, the curves are for different stretching temperatures. The corresponding parameters from the four figures are summarized in Tables I

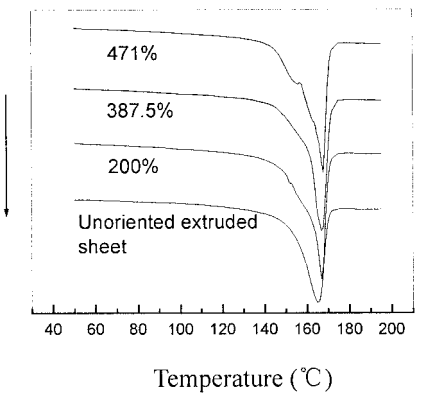

Figure 2 DSC curves of samples stretched at different tensile ratios at 140°C and 150 mm/min.

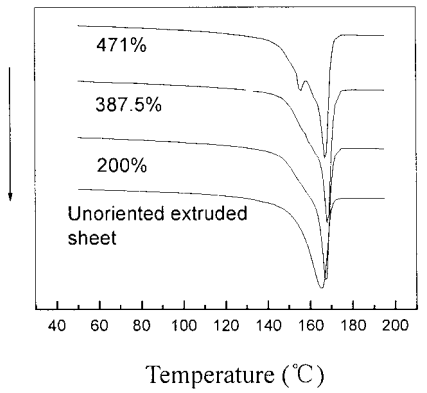

Figure 3 DSC curves of samples stretched at different tensile ratios at 140°C and 300 mm/min.

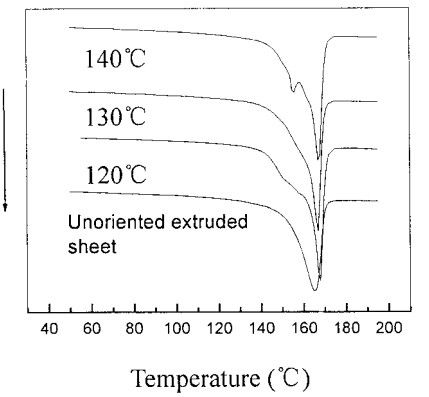

Figure 5 DSC curves of different stretching temperatures at a tensile velocity of 300 mm/min and at a tensile ratio of 471%.

and II, where ΔT refers to the temperature gap (°C) between the onset and end of the melting process as indicated in the DSC heating scans, the melting temperature (T_m) is the higher temperature at which the larger peak is located, and ω_c is the DSC crystallinity.

Many researchers have observed two or more endothermic peaks on the DSC thermograms of iPP treated under different conditions, but the location and interpretation of the peaks have not always been consistent. For example, Turner-Jones et al.[10] gave the first report on the influence of stretching on $\beta \leftrightarrow \alpha$ modification transformation in 1964. Later researchers took the viewpoint that the reorganization induced by strain was the main cause of the fast strain hardening of β modification after yield; that is, in the course of stretching, the transformation of β modification to α modification took place.[22] These researchers also believed that a larger tensile ratio and a higher tensile temperature were beneficial for $\beta \leftrightarrow \alpha$ transformation and the perfection of α modification.

It can be seen in Figures 2 and 3 that at the largest tensile ratios, a shoulder or minor peak appears in the DSC heating scans of about 155°C, which is believed to represent the PP β crystal.[23] The melting point of the main peak, maintained around 167°C, characterizes PP α crystal. On the basis of the following WAXD results, which lack the characteristic (300) diffraction peak, as shown in Figure 6, and DSC heating curves, it can safely be concluded that even though β crystals were not formed, the crystalline structure did change during the hot stretching.

The minor peak became more distinct when the tensile ratio was 471%, but it was not observed when the stretching velocity was higher (450 mm/min). Accordingly, like for what happened in the isothermal crystallization of PP, the structural change indicated by DSC was evident only under limited conditions.

When the tensile velocities were relatively low, the parameters calculated from DSC information followed clear trends. With an increasing tensile ratio, T_m, ΔH_f, and ω_c increased, whereas ΔT decreased congruently. Under the same conditions of stretching velocities and temperatures, a larger tensile ratio means a longer stress-induced crystallization process, resulting in more complete crystals and higher crystallinity.

When the tensile velocity was 450 mm/min, the trend was not so clear. As can be seen in Table I, when the tensile ratio increased, ΔT, ΔH_f, and the corresponding value of ω_c reached a maximum when the tensile ratio was 388% and then decreased. Considering the minor peaks in the DSC thermograms in Figures 2 and 3, we believe that under conditions of high temperatures, tensile velocities, and tensile ratios, that is, rigorous crystallization conditions, some imperfect α crystals collapse and simultaneously reorganize into crystals with thermal properties different from those of pure α modification. The minor peak, or sometimes a shoulder, then emerges and deviates from the trend shown at lower velocities.

With respect to an unoriented extruded sheet, stretching had a great influence on the crystallinity. After the MD stretching, the crystallinity increased on average by about 20% and, under some special condi-

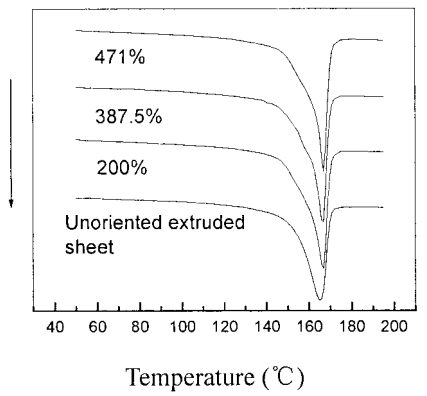

Figure 4 DSC curves of samples stretched at different tensile ratios at 140°C and 450 mm/min.

TABLE I
Index of Crystallinity and Related Parameters of BOPP Specimens Hot-Stretched and Deformed at 140°C, Obtained from DSC Measurements

Controlling parameters		Property parameter			
Tensile velocity	Tensile ratio (%)	ΔT (°C)	T_m (°C)	ΔH (J/g)	ω_c (%)
	200	37.50	167.20	68.84	49.9
150	388	37.34	167.41	73.11	53.0
	471	36.43	167.82	74.50	54.0
	200	38.22	167.50	69.38	50.3
300	388	37.14	168.42	71.44	51.8
	471	35.35	167.44	71.27	51.6
	200	35.35	166.72	65.64	47.6
450	388	41.43	166.64	70.61	51.2
	471	40.07	167.08	68.75	49.8
0	0	38.21	165.43	58.64	42.5

tions, induced crystal reorganization. Because of the different properties of the crystal modification of PP and the higher crystallinity after stretching, it was important to carefully control the stretching parameters.

WAXD

Figure 6 shows the WAXD patterns of an extruded sheet without stretching and a stretched sheet. The sheet without stretching gave a pure α-crystal diffraction pattern with high (110), (040), (130), and (131)–(041) diffraction intensities, with the 2θ angle located at 13.72, 16.9, 18.38, 20.61, and 21.55°. After a period of stretching at 140°C, the notable reflection profile located at about 21.55° of (131)–(041) disappeared, and this agreed with Alberola et al.'s[24] observation. This was interpreted as a suggestion that the stretching could lead to a preferential orientation intermediate between 0 and 90°with respect to the drawing direction, supporting the DSC results for the aforementioned structural changes but not agreeing with the presence of β crystals.

Simultaneously, the *d*-spacing of these crystal planes also changed regularly, as shown in Figure 6. For example, the *d*-spacing of the (110) plane from the WAXD test changed from 6.44 Å for PD382 to 6.33 Å for H323E5 and 6.31 Å for H313E5, and this was also true for the (040) and (130) planes. Moreover, structural changes in the same direction are indicated by the quite close peak location of the stretched samples.

In comparison with the sample not stretched, the stretched samples were greatly reduced with respect to the noncrystal diffusion. This indicated a transformation into the crystal phase during stretching and crystal reorganization, and the crystallinity of the tested samples was raised in agreement with the DSC crystallinity results.

CONCLUSIONS

Through a simulation of the hot stretching in the processing of BOPP films in the MD, we found that at higher tensile ratios, a shoulder or minor peak appeared in the DSC heating scans at about 155°C. This was attributed to changes in the aggregation state, especially in the crystalline structure during hot stretching. The minor peak was more distinct when the tensile ratio was 471%. When the tensile velocities were relatively lower, the parameters from DSC heating scans followed a clear trend with an increasing tensile ratio. T_m, ΔH_f, and ω_c increased, whereas ΔT decreased congruently. However, when the tensile velocity was 450 mm/min, the changing trend was not so clear. After the MD hot stretching, the crystallinity increased on average by about 20%. The WAXD patterns of a sample without stretching and stretched sheets showed that the structural changes and the

TABLE II
Index of Crystallinity and Related Parameters of BOPP Specimens Hot-Stretched and Deformed at a Tensile Velocity of 300 mm/min and at a Tensile Ratio of 471%, Obtained from DSC Measurements

	Property parameter			
Stretching temperature (°C)	ΔT (°C)	T_m (°C)	ΔH (J/g)	ω_c (%)
120	38.93	167.71	75.64	54.8
130	35.00	166.82	67.90	49.2
140	35.35	167.44	71.27	51.6
Unorientedextrudedsheet	38.21	165.43	58.64	42.5

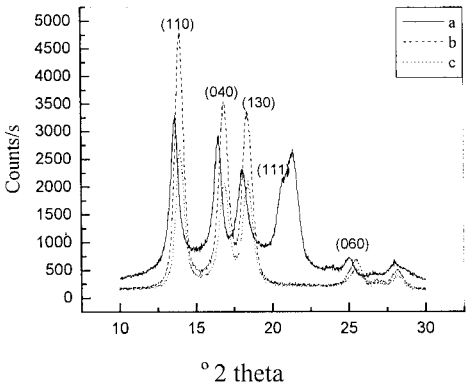

Figure 6 WAXD patterns of (a) an unoriented extruded sheet, (b) a sample stretched at 140°C at a tensile velocity of 150 mm/min and at a tensile ratio of 471%, and (c) a sample stretched at 140°C at a tensile velocity of 300 mm/min and at a tensile ratio of 471%.

reflection profile located at about 21.55° (2θ) of (131)–(041) disappeared after the stretching at 140°C, and the *d*-spacing of the crystal (110), (040), and (130) planes also became larger. The results affirmed that the β crystal did not come into being during the entire MD hot-stretching process.

References

1. Yang, W.; Li, Z.-M.; Feng, J.-M.; Yu, G.-P.; Shi, W.; Yang, M.-B. Polym Mater Sci Eng 2002, 20(3), 10.
2. Yang, W.; Li, Z.-M.; Feng, J.-M.; Yu, Q.-S.; Yang, M.-B. Chin Plast 2001, 15(10), 43.
3. Yang, M.-B.; Yang, W.; Li, Z.-M.; Feng, J.-M. Polym Mater Sci Eng 2001, 19(5), 153.
4. Zhenhua, S.; Fusheng, Y.; Yuchen, Q. Polymer 1991, 32, 1059.
5. Morrow, D. R. J Macromol Sci Phys 1969, 3, 53.
6. Shi, G. Y.; Huang, B.; Cao, Y. Makromol Chem 1986, 187, 643.
7. Rybnikar, F. J Macromol Sci Phys 1991, 30, 201.
8. Varga, J.; Schulek-Toth, F.; Ille, A. Colloid Polym Sci 1991, 269, 655.
9. Padden, F. J., Jr.; Keith, H. D. J Appl Phys 1959, 30, 1479.
10. Turner-Jones, A.; Aizlewood, J. M.; Beckeet, D. R. Makromol Chem 1964, 75, 134.
11. Lovinger, A. J.; Chua, J. O.; Gryte, C. C. J Polym Sci Polym Phys Ed 1977, 15, 641.
12. Dragaum, H.; Muschik, H. J. J Polym Sci Polym Phys Ed 1977, 15, 1779.
13. Leugering, H. J. Makromol Chem 1967, 109, 204.
14. Turner-Jones, A.; Cobbold, A. J. J Polym Sci 1968, 6, 539.
15. Garbarczyk, J.; Sterzyski, T.; Paukzta, D. Polym Commun 1989, 30, 153.
16. Li, J. X. Polymer 1999, 40, 2085.
17. Li, J. X. Polymer 1999, 40, 2089.
18. Yang, J. Mod Plast Process Appl 1998, 10(4), 60.
19. De Vries, A. Pure Appl Chem 1981, 53, 1011.
20. Renjie, W. Modern Analyzing Techniques Used In Polymers (in Chinese); Shanghai Science and Technology: Shanghai, China, 1986.
21. Yuksekkalayci, C. Polym Eng Sci 1999, 39, 1217.
22. Strobel, J.; Nam, S. J Appl Polym Sci 1981, 42, 159.
23. Aboulfaraj, M.; Ulrich, B.; Dahoun, A.; G'Sell, C. Polym J 1993, 23, 4817.
24. Alberola, N.; Fugier, M.; Petit, D.; Fillon, B. J Mater Sci 1995, 30, 860.